

# Electrochemical characteristics of semi conductive silicon anode for lithium polymer batteries

Arenst Andreas Arie · Wonyoung Chang ·  
Joong Kee Lee

Received: 11 December 2008 / Accepted: 13 April 2009 / Published online: 5 May 2009  
© Springer Science + Business Media, LLC 2009

**Abstract** In this paper, the electrochemical characteristics of semi conductive silicon thin films (n-type and p-type silicon) anodes integrated with the solid polymer electrolyte for lithium polymer batteries were investigated. The charge/discharge cycling tests revealed that the phosphorus-doped n-type silicon electrode shows the most stable cyclic performance after the 40<sup>th</sup> cycle and still maintains a reversible specific capacity of about 2,500 mAh/g. The enhanced electrochemical performance of the doped silicon anode was attributed to the enhancement of its electrical conductivity, which was further confirmed by impedance spectroscopy and surface analysis by XPS.

**Keywords** Lithium polymer battery · Thin films · Impedance · Semi conductive

## 1 Introduction

The future applications in the field of telecommunications, electronics and hybrid electric vehicles (HEVs) require batteries with a much higher specific capacity and safer operation as their power and energy supply [1–3]. The current technology of lithium batteries is constrained by

their limited specific capacity, because of the use of graphite as anode materials (theoretical capacity of 372 mAhg<sup>-1</sup>). Silicon-based lithium polymer batteries satisfying higher capacity and safety issue could be one of the alternatives to meet the future demand [4, 5].

Silicon has been considered as one of the most attractive candidates to replace the graphite or carbon-based anode, because of its potential high capacity of 4,200 mAhg<sup>-1</sup>. The main problem that must be alleviated for the commercial application of intrinsic silicon as an anode material is its poor cycle performance. It is already known that one reason for poor cycle performance of silicon anode is its low electronic conductivity [6].

In an effort to enhance the electronic conductivity of silicon thin film anode, the doping of hetero-atoms into the silicon matrix could be explored, as in the case of the carbon electrode [7]. There have been a few reports which focused on the doping of hetero-atoms, such as boron and phosphorus, into the silicon host matrix to produce p-type and n-type silicon thin film anodes, respectively, with a high specific capacity, however most of them were based on the standard liquid electrolyte system [8–10]. Therefore, in the present work, we studied the application of two types of semi-conductive silicon thin film (n-type and p-type Si) as anode materials integrated with a gel polymer as the solid electrolyte for lithium polymer batteries. The influence of boron and phosphorus doping on electrochemical performance of silicon anodes was studied with electrochemical measurements and XPS analysis.

## 2 Experimental

Three types of silicon thin films were used in this experiment; i.e. intrinsic or un-doped silicon, phosphorus doped n-type silicon and boron doped p-type silicon. All of

A. Andreas Arie · W. Chang · J. Kee Lee (✉)  
Advanced Energy Materials Processing Laboratory, Battery Research Center, Korea Institute of Science and Technology, P.O. BOX 131, Cheongryang, Seoul 130-650, Korea  
e-mail: leejk@kist.re.kr

A. Andreas Arie  
e-mail: arenst@yahoo.com

A. Andreas Arie  
Energy Conversion Technology Division,  
University of Science and Technology,  
Daejeon, Korea

films were prepared by radio frequency coupled plasma enhanced chemical vapor deposition (rf-PECVD) onto a 10  $\mu\text{m}$  thick  $2 \times 2 \text{ cm}^2$  copper foil. The CVD reactor was evacuated down to a base pressure of  $10^{-5}$  torr and the working pressure of  $8.0 \times 10^{-2}$  torr was maintained by argon gas (Ar). Intrinsic silicon thin film was produced by feeding silane gas ( $\text{SiH}_4$ ) as the Si source gas into the argon gas inside the reactor chamber. The n-type doping of the silicon thin film was accomplished by introducing phosphine gas ( $\text{PH}_3$ ) into the argon gas and silane ( $\text{SiH}_4$ ) gas with a feeding mole ratio between silane and phosphine of 1%. Finally, for the p-type doped silicon, di-borane gas ( $\text{B}_2\text{H}_6$ ) was used with a feeding mole ratio of silane to di-borane of 5%. The deposition time, radio frequency (rf) power and substrate temperature for all of the above processes were fixed at 30 min, 200 W and 150°C, respectively. The resulted thin films were found to have thickness about 400 nm (shown by SEM).

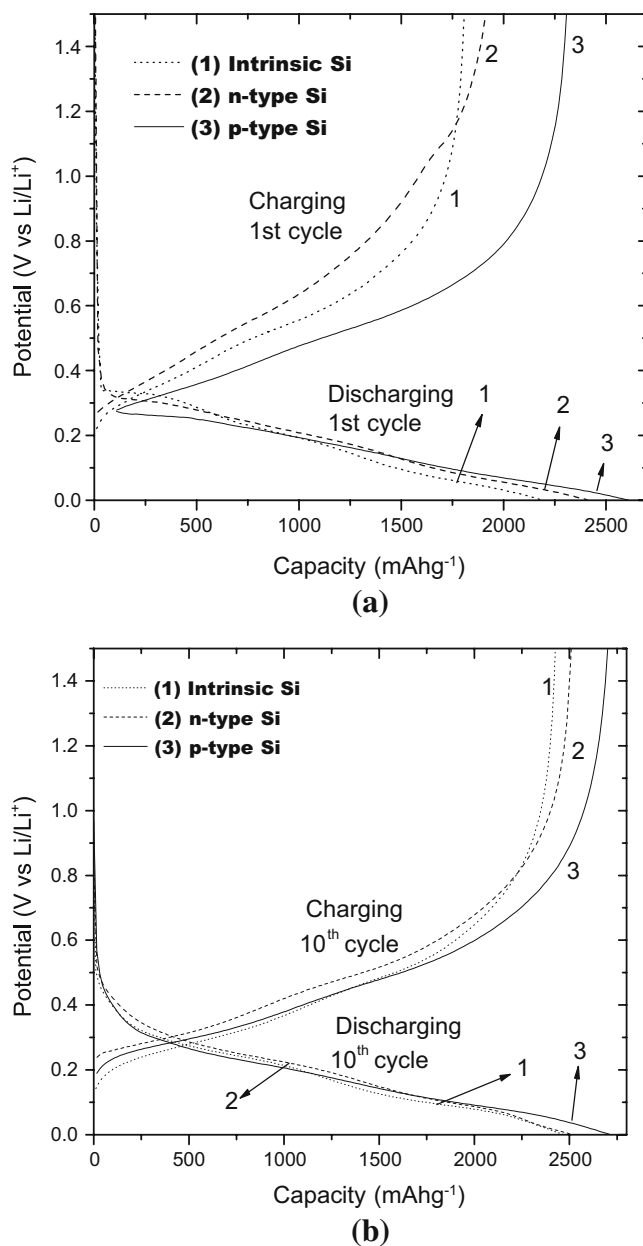
For electrochemical study of each silicon films, half cells were fabricated with silicon film as the working electrode and lithium metal foil as the counter electrode using a gel polymer electrolyte as a separator. The gel polymer electrolyte was prepared by solution casting. Initially, 1.5 g of lithium trifluoro methane sulfonate ( $\text{LiCF}_3\text{SO}_3/\text{LITFS}$ ), EC and PC were mixed in the appropriate ratios with PAN and PVDF (9:1 w %) under magnetic stirring at 300 rpm for 5 h until a homogeneous solution was obtained. Subsequently, the polymer electrolyte was maintained at a temperature of 140–150°C for 2 h using a hot plate in order to obtain the gel polymer. This gel polymer was then slowly dried at 60°C, in order to obtain a uniform solid membrane and, finally, the gel membranes were dried in a vacuum oven for 24 h before assembling the cells.

The cells were fabricated in a dry room (max. moisture less than 5%) with the gel polymer electrolyte being placed between the working electrode and counter electrode. Each half cell was then galvanostatically charged/discharged at 0.3 C rates with cut-off voltages in the range of 0.001 V and 1.5 V versus  $\text{Li}/\text{Li}^+$  (Maccor Series 4000). Impedance measurements for each sample were carried out over the frequency range of 0.1 to  $10^6$  Hz with amplitude of 5 mV (Zahner Electrik IM6). All of the electrochemical tests were carried out at room temperature.

Cells with the above-mentioned silicon anodes (p-type, n-type and intrinsic) also prepared for X-ray photoelectron spectroscopy (XPS) analysis (VG Scientific ESCALAB 200R). After the first cycle of the charge/discharge tests, each anode was separated from its fabricated cell in a dry chamber, washed several times with dimethyl carbonate (DMC) and then analyzed in an XPS vacuum chamber without any contact with the surrounding air. The analysis of the samples was performed with respect to F 1 s and O 1 s. The conductivity of bulk silicon film was measured by using four point probe method.

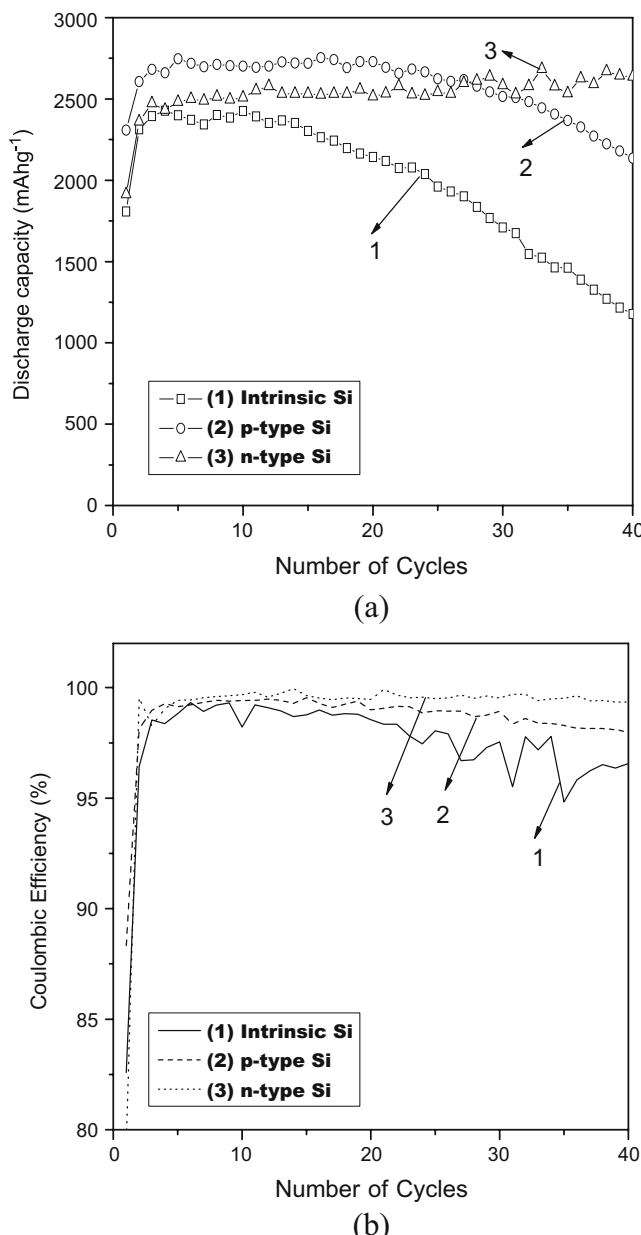
### 3 Results and discussion

Figure 1 displays the charge/discharge curves at 0.3 C rates of the intrinsic, phosphorus (n type) and boron doped (p type) silicon electrodes at the 1<sup>st</sup> and 10<sup>th</sup> cycles. At the 1<sup>st</sup> cycle (Fig. 1(a)), it was observed that the voltage profiles and specific capacity of the p type silicon electrode are higher than those of the other silicon samples. The first discharge capacity of the p-type silicon electrode is  $2,613 \text{ mAhg}^{-1}$  and its first charge capacity is  $2,308 \text{ mAhg}^{-1}$ . The intrinsic silicon electrode shows discharge and charge



**Fig. 1** Charge/discharge curves at 0.3 C rates for the three kinds of silicon thin film electrode at the (a) 1<sup>st</sup> cycle (b) 10<sup>th</sup> cycle

capacities of  $2,188 \text{ mAhg}^{-1}$  and  $1,807 \text{ mAhg}^{-1}$ , respectively, while the n-type silicon electrode has a first discharge capacity of  $2,412 \text{ mAhg}^{-1}$  and charge capacity of  $1,913 \text{ mAhg}^{-1}$ . Thus, we can say that the phosphorus and boron doping has successfully elevated the specific capacity of the silicon electrode. In addition, all of the silicon electrodes possessed charge capacities lower than their corresponding discharge capacities at the first cycle, which is attributed to the formation of an SEI film on their surface. In the initial discharge at the first cycle, the potential decreased rapidly to plateaus observed near the voltage



**Fig. 2** The profiles of (a) discharge capacity and (b) coulombic efficiency versus cycle number for three kinds of silicon thin film electrode

range of about  $0.25 \text{ V}$ – $0.35 \text{ V}$  for all three kinds of silicon electrode (Fig. 1(a)). If we look carefully at the end of the 10<sup>th</sup> cycle, the potential plateaus observed in the 1<sup>st</sup> cycle completely disappear for all three silicon samples (Fig. 1(b)). As a result, the specific capacity of the silicon electrode is larger than that obtained in the 1<sup>st</sup> cycle.

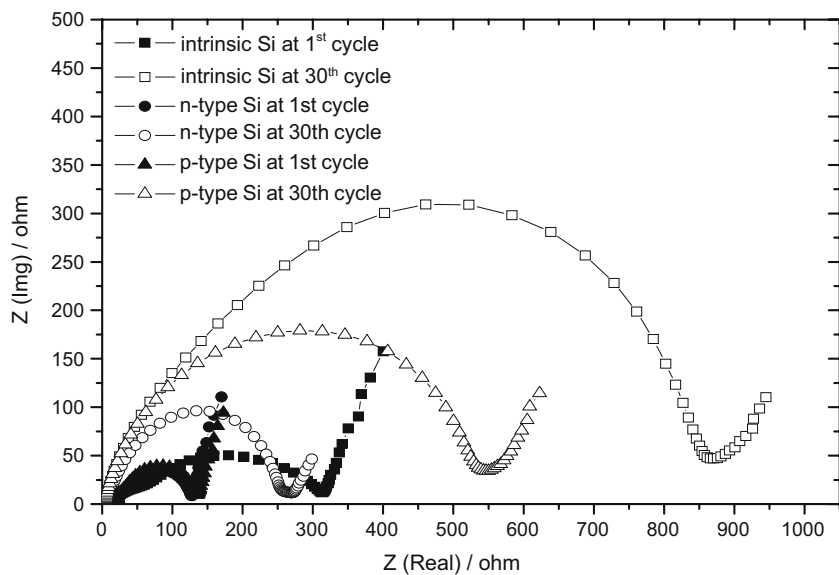
Figure 2 compares the cycle performance of the silicon electrodes in terms of their discharge capacity and coulombic efficiency in the voltage range between  $0.001$  and  $1.5 \text{ V}$  versus  $\text{Li}/\text{Li}^+$  at  $0.3 \text{ C}$  rates. As shown in Fig. 2(a), a significant improvement was achieved with the n-type silicon electrode; its capacity remains above  $2,500 \text{ mAhg}^{-1}$  up to the 40<sup>th</sup> cycle. In addition, it shows the most stable cyclic profiles and highest coulombic efficiency after the 10<sup>th</sup> cycle among the three kinds of silicon electrode (Fig. 2(b)). On the other hand, the capacity of the intrinsic silicon electrode fades rapidly after the 20<sup>th</sup> cycle. This fading capacity phenomenon can also be found in the cyclic performance of the p-type silicon electrode, in which the capacity begins to drop after the 30<sup>th</sup> cycle. However, the p-type silicon electrode still gives better electrochemical performance than the intrinsic silicon electrode, since it shows a higher coulombic efficiency, as depicted in Fig. 2(b). Table 1 summarizes the electronic conductivity, initial capacity and capacity retention after the 40<sup>th</sup> cycle as a function of the type of impurity/dopant agent (P or B). As shown in Table 1, higher capacity retention after the 40<sup>th</sup> cycle was obtained in the case of the Si anode with its higher electrical conductivity. Thus, the increase in electronic conductivity by doping may contribute to the stability of the cyclic performance of the silicon anode. Based on these observations, it can be said that phosphorus as well as boron doping enhances the electrochemical properties of the silicon electrode. In addition, the n-type silicon anode exhibits the largest capacity and the most stable performance.

In order to have more insight into the enhanced electrochemical characteristics, especially to examine the conductivity of the Li ions in the Si electrodes, AC impedance measurements were performed for all three silicon electrodes after the first and thirtieth cycles, which shown in Fig. 3.

**Table 1** The effects of the dopants on the capacity and sheet resistivity of the doped silicon electrodes.

|              | Bulk conductivity ( $\Omega \cdot \text{cm}$ ) <sup>-1</sup> | Initial capacity at 1 <sup>st</sup> cycle (mAhg <sup>-1</sup> ) | Capacity retention after the 40 <sup>th</sup> cycle (%) |
|--------------|--|---|---|
| intrinsic Si | $10^{-6}$ – $10^{-8}$  | 2,188   | 47%   |
| n-type Si    | $9.8 \cdot 10^{-1}$  | 2,412   | 95%   |
| p-type Si    | $4.8 \cdot 10^{-3}$  | 2,613   | 78%   |

**Fig. 3** Nyquist plots of three kinds of silicon thin film electrode after the 1<sup>st</sup> and 30<sup>th</sup> cycles

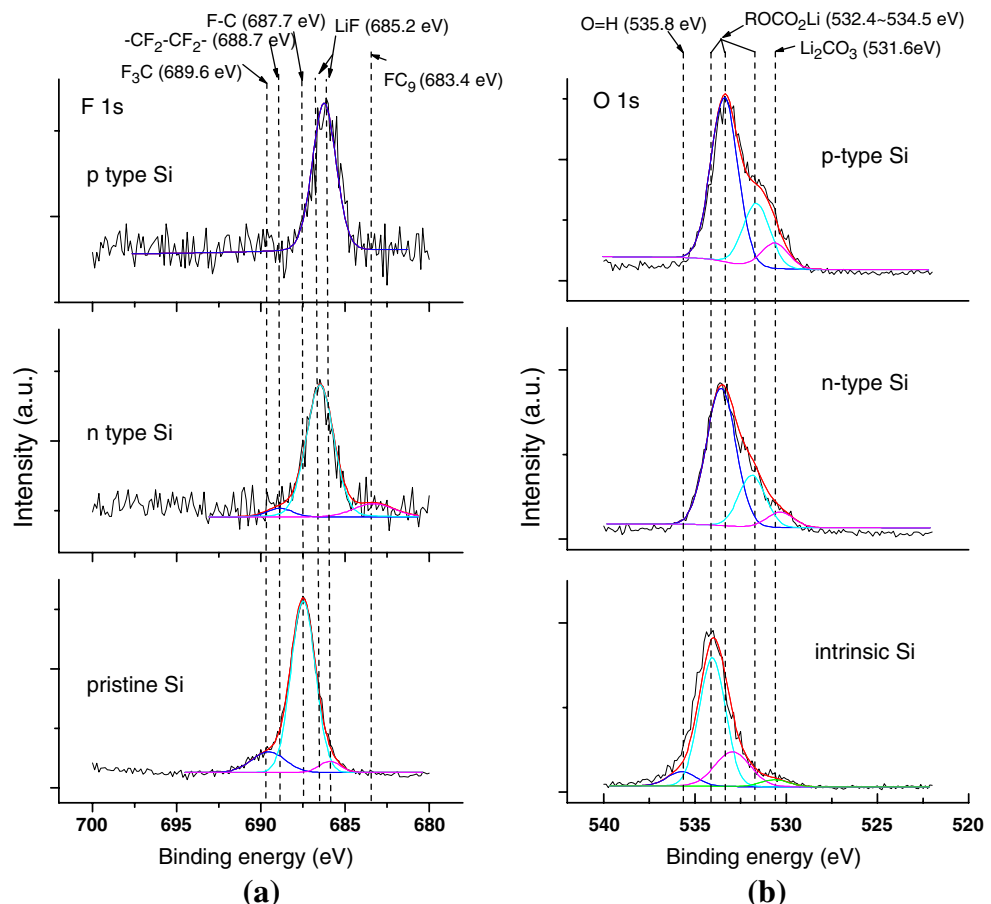


At the 1<sup>st</sup> cycle, all of spectra consist of two well-defined semicircles, followed by linear portion. The first semicircle at high frequency region is correlated with the formation of passivation film on the surface, and the second semicircle at middle frequency region is caused by charge transfer of lithium ion at interface. At the 1<sup>st</sup> cycle, the interfacial

impedances for both doped silicon electrodes were obviously smaller than that of the intrinsic silicon electrode, and only a small difference in impedance was observed between n-type and p-type silicon electrodes.

With increasing the number of cycle from the 1<sup>st</sup> to the 30<sup>th</sup>, it was shown that the diameters of the high frequency-

**Fig. 4** F 1 s and O 1 s XPS spectra for surface of silicon thin film anodes after the 1<sup>st</sup> cycle



combined semicircles get increased for all silicon electrodes. However, unlike the 1<sup>st</sup> cycle, n-type silicon electrode underwent much smaller increase in impedance compared to the p-type silicon electrode. We suspect that the enhanced electronic conductivity of silicon electrode by doping mechanism, especially n-type doping, can play a positive role for more lithium ions to easily transfer at the electrode/electrolyte interface, thus giving the higher capacity. But, further investigation is still required for this topic.

Figure 4 shows the XPS spectra of F 1 s and O 1 s for the surface of silicon after the first cycling. After the deconvolution of the peaks for the F 1 s spectra (Fig. 4(a)), it was found that the doped silicon thin films (n type and p type) showed a strong peak from LiF at a binding energy of 685.4 eV. It should be noted that the binding energy of LiF contained on the surface of both doped Si electrodes (n type and p type) is higher than that of the intrinsic Si, which implies that the more stable layer has been formed. This stable layer formed on the interface contributes to the maintenance of the lower impedance of the doped silicon electrode [11, 12] and, hence, results in enhanced electrochemical performance. Moreover, the n type silicon electrode shows a binding energy which is slightly higher than that of the p type one, which means that the more stable layer has been formed in the case of the n type Si electrode. Figure 4(b) shows that besides LiF, some compounds are formed on the surface of silicon such as Li<sub>2</sub>CO<sub>3</sub> and Li alkyl carbonate.

Based on the results obtained from impedance spectroscopy and XPS data, which support each other, it can be said that more enhanced and more stable cyclic performance can be obtained with doped silicon electrodes. From the experimental results, it is concluded that the enhanced electronic conductivity plays an important role in providing a favorable electrochemical performance for the lithium ion insertion/extraction reaction.

#### 4 Conclusions

In this paper, the effect of phosphorus and boron doping on the electrochemical performance of Si thin film anodes was investigated. The presence of the doped atoms resulted in

the excellent cycle performance and high capacity of the silicon anode. This enhanced electrochemical performance was mainly attributed to the increased conductivity of the Li ions and stable layer formed on the surface of the doped silicon anode. On the other hand, in the case of the intrinsic silicon electrode, the interfacial impedance was relatively high due to the formation of an unstable surface layer, which would lead to anode polarization and ultimately result in poor cyclic performance and low capacity retention.

**Acknowledgement** The authors thank Mr. Ji Hun Park for XPS analysis and helpful discussion. This research was supported by a grant(code #05K1501-01920) from ‘Center for Nanostructured Materials Technology’ under ‘21st Century Frontier R&D Programs’ of the Ministry of Science and Technology, Korea.

#### References

1. O. Bitsche, G. Gutmann, J. Power Sources **127**, 8–15 (2004). doi:[10.1016/j.jpowsour.2003.09.003](https://doi.org/10.1016/j.jpowsour.2003.09.003)
2. J.M. Tarascon, M. Armand, Nature **414**, 359–499 (2001). doi:[10.1038/35104644](https://doi.org/10.1038/35104644)
3. Y. Nishi, J. Power Sources **100**, 101–106 (2001). doi:[10.1016/S0378-7753\(01\)00887-4](https://doi.org/10.1016/S0378-7753(01)00887-4)
4. S. Dhameja, *Electric Vehicle Battery System* (Newnes-Butterworth Heinemann, Boston- Oxford, 2002), pp. 13–14
5. F.B. Dias, L. Plomp, J.B.J. Veldhuis, J. Power Sources **88**, 169–191 (2000). doi:[10.1016/S0378-7753\(99\)00529-7](https://doi.org/10.1016/S0378-7753(99)00529-7)
6. D. Larcher, C. Mudalige, A.E. George, V. Porter, M.K. Gharghouri, J.R. Dahn, Solid State Ion **122**, 71 (1999). doi:[10.1016/S0167-2738\(98\)00557-8](https://doi.org/10.1016/S0167-2738(98)00557-8)
7. Y.P. Wu, E. Rahm, R. Holze, Electrochim. Acta **47**, 3491–3507 (2002). doi:[10.1016/S0013-4686\(02\)00317-1](https://doi.org/10.1016/S0013-4686(02)00317-1)
8. S. Ohara, J. Suzuki, K. Sekine, T. Takamura, J. Power Sources **136**, 303–306 (2004). doi:[10.1016/j.jpowsour.2004.03.014](https://doi.org/10.1016/j.jpowsour.2004.03.014)
9. M. Uehara, J. Suzuki, K. Tamura, K. Sekine, T. Takamura, J. Power Sources **146**, 441–444 (2005). doi:[10.1016/j.jpowsour.2005.03.097](https://doi.org/10.1016/j.jpowsour.2005.03.097)
10. T. Ishihara, M. Nakasu, M. Yoshio, H. Nishiguchi, Y. Takita, J. Power Sources **146**, 161–165 (2005). doi:[10.1016/j.jpowsour.2005.03.110](https://doi.org/10.1016/j.jpowsour.2005.03.110)
11. T. Sotomura, K. Adachi, M. Taguchi, M. Iwaku, T. Tatsuma, N. Oyama, J. Power Sources **81-82**, 199 (1999). doi:[10.1016/S0378-7753\(98\)00211-0](https://doi.org/10.1016/S0378-7753(98)00211-0)
12. N.S. Choi, K.H. Yew, K.Y. Lee, M. Sung, H. Kim, S.S. Kim, J. Power Sources **161**, 1259 (2006). doi:[10.1016/j.jpowsour.2006.05.049](https://doi.org/10.1016/j.jpowsour.2006.05.049)